

University of California, Davis

**Modeling Discontinuities and their
Evolution within Finite Elements:
Application to Material Interfaces,
3-D Cracks, and Microstructures**



N. Sukumar

UC Davis

Rutgers University, Sept. 7, 2001

Collaborators and Acknowledgments

- X-FEM (3D Cracks): N. Moes, B. Moran, and T. Belytschko (Northwestern University)
 - X-FEM (Material Interfaces and 3D Crack Growth) : D. Chopp (Northwestern University)
 - X-FEM (Microstructure): D. J. Srolovitz, J. Prevoost, and T. J. Baker (Princeton University)
-
- Mark Miodownik and Elizabeth Holm are thanked for providing the Potts model code



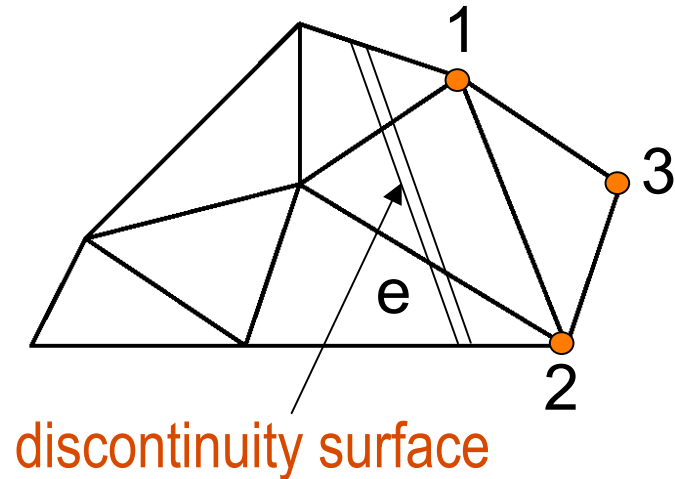
Outline

- Modeling Discontinuities in Finite Elements
- Extended Finite Element and Level Set Methods
- Applications
 - Material Interfaces
 - Three-Dimensional Cracks
 - Polycrystalline Microstructures
- Conclusions



Modeling Discontinuities in Finite Elements

- Classical Approach (FE)
Crack discontinuity modeled by the mesh; use of **quarter-point element** leads to better accuracy



- Embedded Discontinuities
 - Weak discontinuity: $\hat{\mathbf{a}}^h = \hat{\mathbf{a}} + \hat{\mathbf{a}}^{enh}$
(Ortiz et al., 1987, Belytschko et al., 1988)
 - Strong discontinuity: $\mathbf{u}^h = \bar{\mathbf{u}} + [\mathbf{u}]H_{\mathcal{S}}(\mathbf{x})$
(Simo et al., 1993)

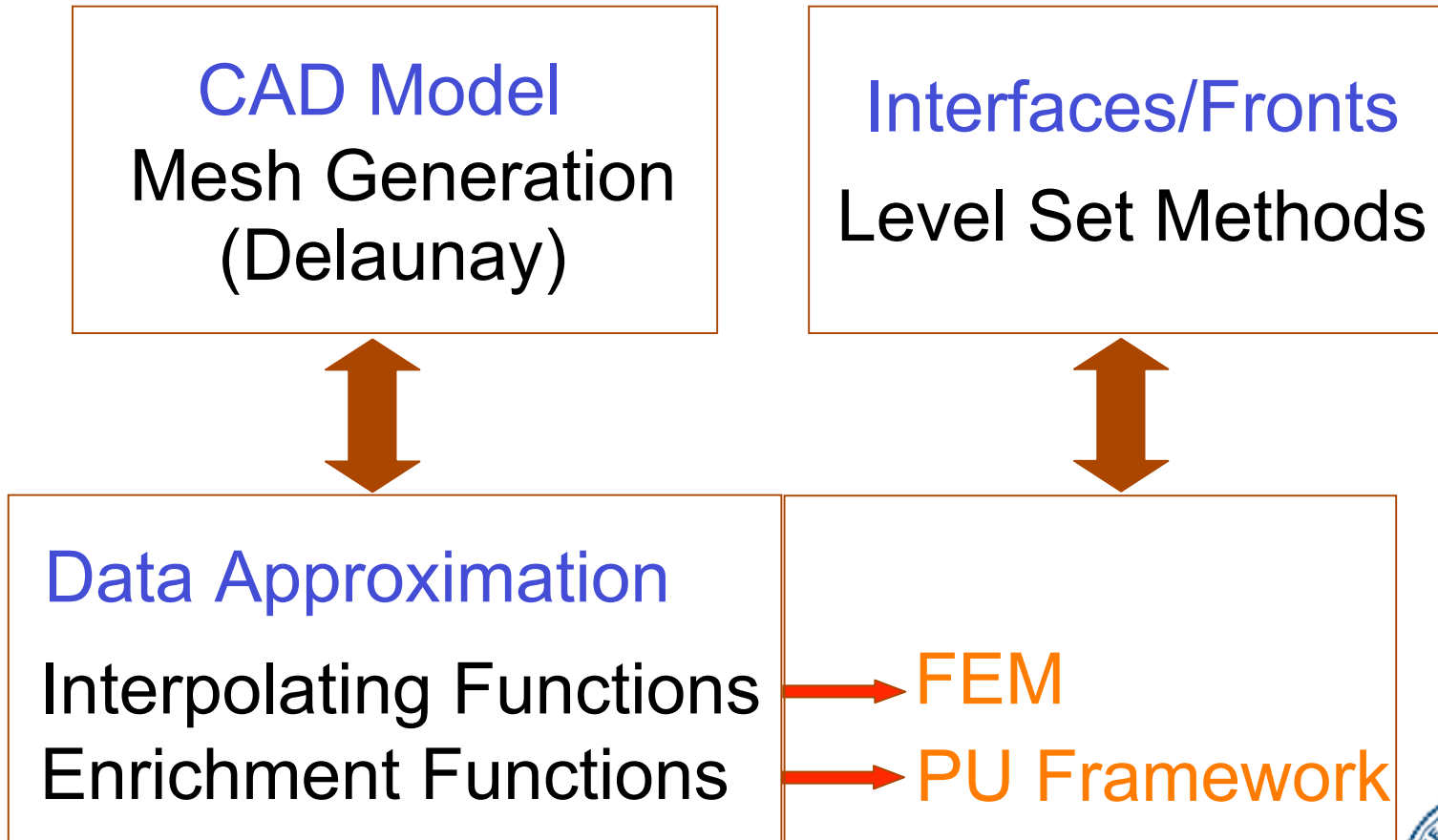


Strong Discontinuity Approach

- Displacement consists of regular and enhanced components, where the enhanced component yields a jump across the discontinuity surface
- Multi-field (assumed strain) variational principle is used
- Enhanced degrees of freedom are statically condensed on each element, which introduces incompatibilities between elements
- Discontinuity surface can only end on element edges
- Mesh dependency exists, and extension to 3-D problems is non-trivial



New Paradigm in Computational Mechanics



Partition of Unity Method (Melenk and Babuska, 1996)

Introduction of a function $f(\mathbf{x})$ in a FE space over a region $D \subset \Omega$ such that the sparsity of the stiffness matrix is retained

Classical Finite Element Approximation

$$u^h(\mathbf{x}) = \sum_I \phi_I(\mathbf{x}) u_I,$$

$$\sum_I \phi_I(\mathbf{x}) = 1, \quad \sum_I \phi_I(\mathbf{x}) \mathbf{x}_I = \mathbf{x}$$



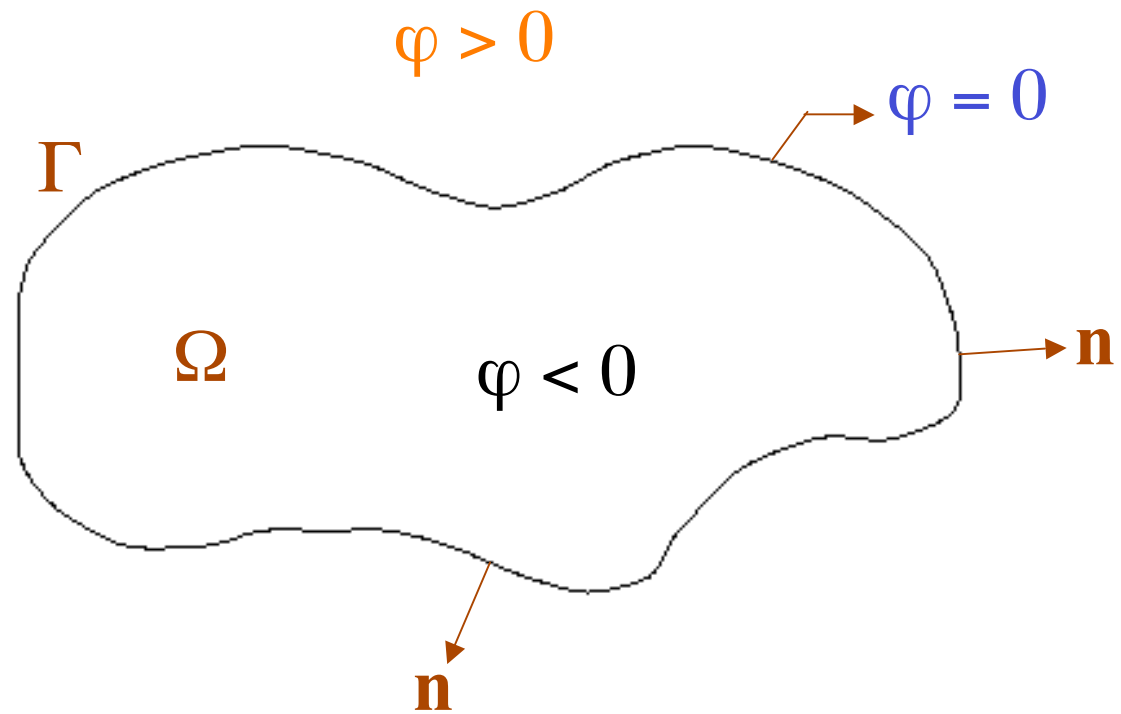
Level Set and Fast Marching Methods (FMM)

- Numerical techniques for tracking moving interfaces, with the interface represented as the **zero level contour** of a function of one higher-dimension
- Hyperbolic equation in terms of level set function $\varphi(\mathbf{x}, t)$ governs the motion of the interface; **FMM** is well-suited for propagation of monotonic fronts (**Sethian, 1996**)

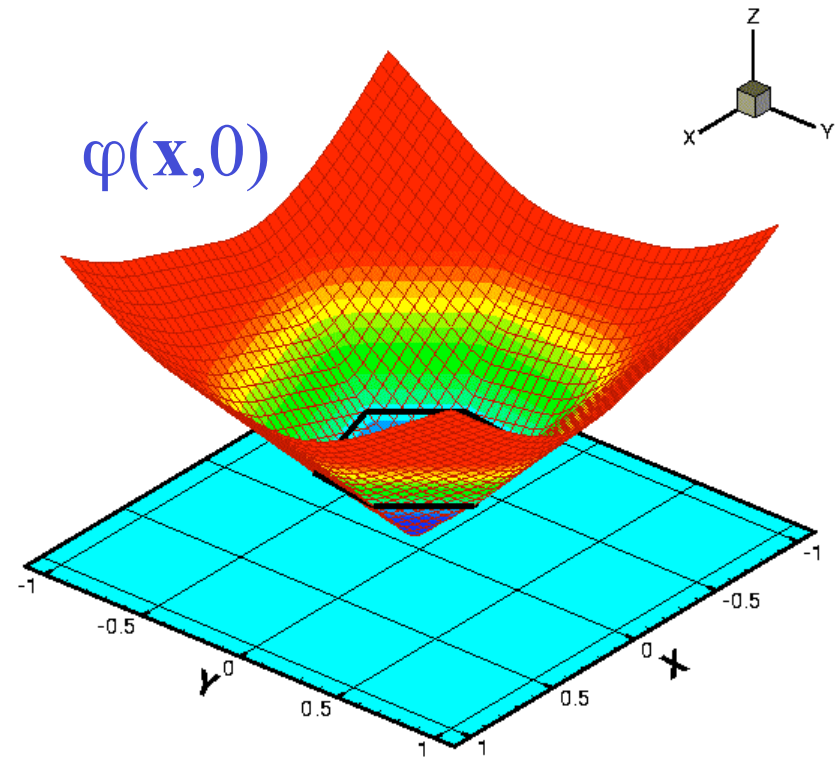
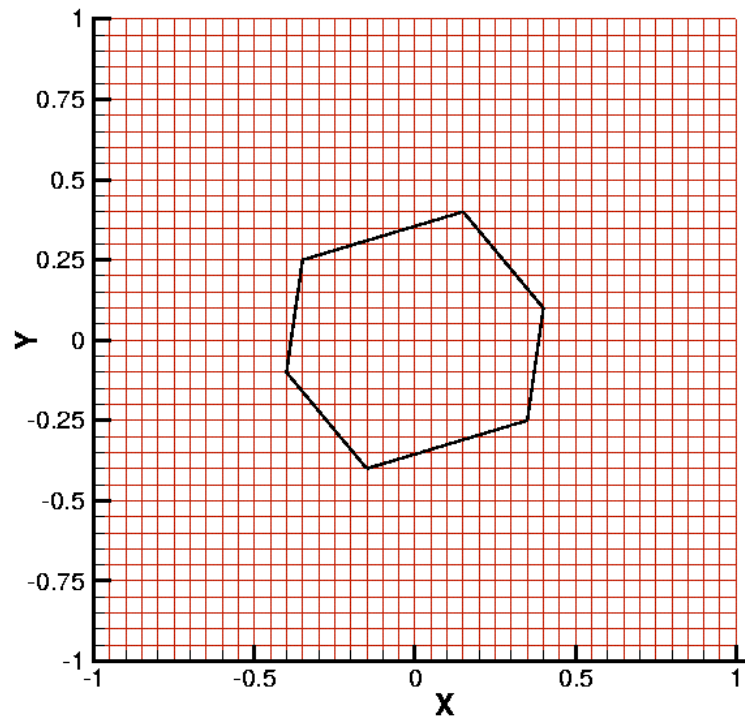
- **Advantages**
 - Computed on a fixed Eulerian grid
 - Handles topological changes in the interface naturally
 - Readily extends to \mathbf{R}^d



Level Set Function



Hexagonal Interface



Extended Finite Element Method (Moes et al, 1999)

- Finite element mesh is used to describe the domain
- Internal boundaries (e.g., cracks, holes, interfaces) are **not** part of the mesh
- Presence of internal boundaries is ensured by enriching the displacement approximation
- **Single-field** variational principle is used, and the stiffness matrix is sparse and symmetric
- Level set and fast marching methods are used to evolve the crack front in 3-D crack applications
- **No remeshing** required for crack growth simulations



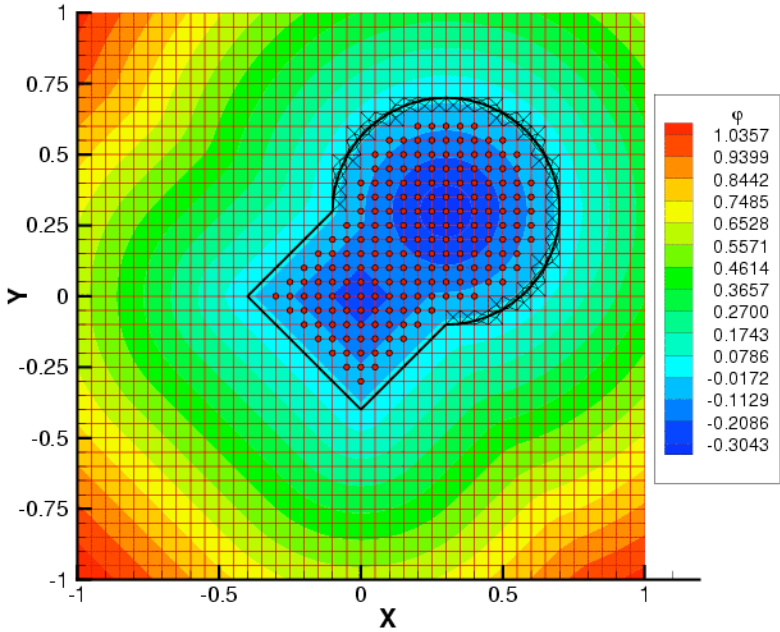
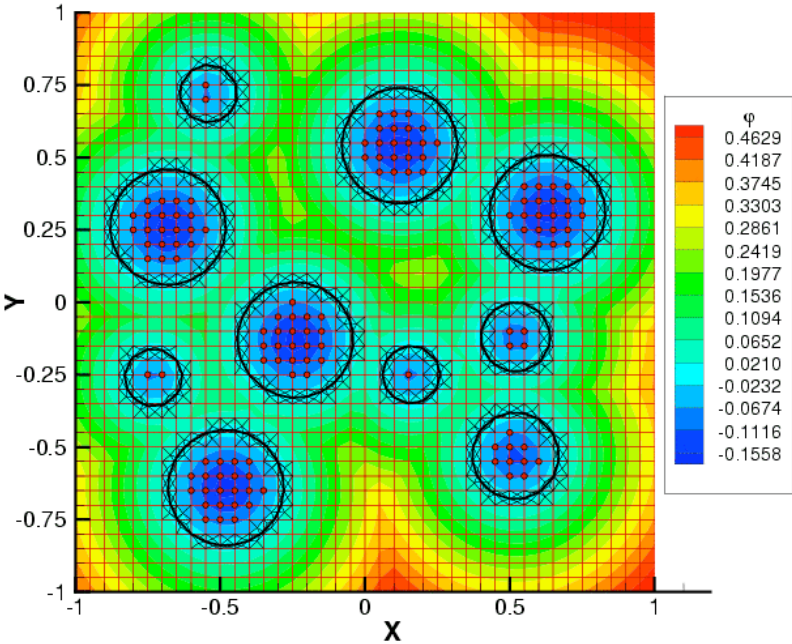
Enriched Displacement Approximation (X-FEM)

$$u_i^h(\mathbf{x}) = \sum_{n_I \in \mathbf{N}} \phi_I(\mathbf{x}) u_{iI} + \sum_{n_J \in \mathbf{N}^c} \phi_J(\mathbf{x}) a_{iJ} \Psi(\mathbf{x})$$

- Choice of the enrichment function $\Psi(\mathbf{x})$ depends on the geometric entity (material interface, crack-tip, crack surface, etc.)
- \mathbf{N}^c is the set of nodes whose support intersects the geometric entity of interest



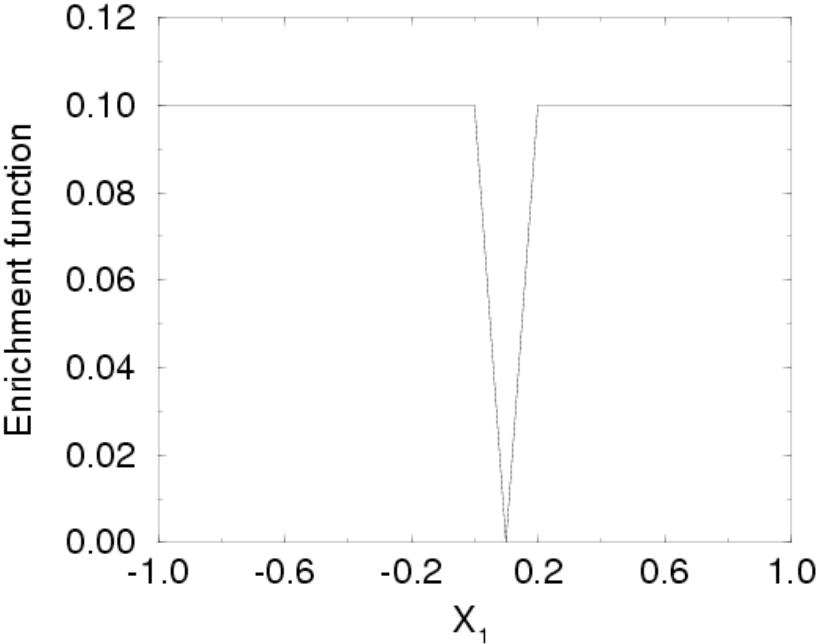
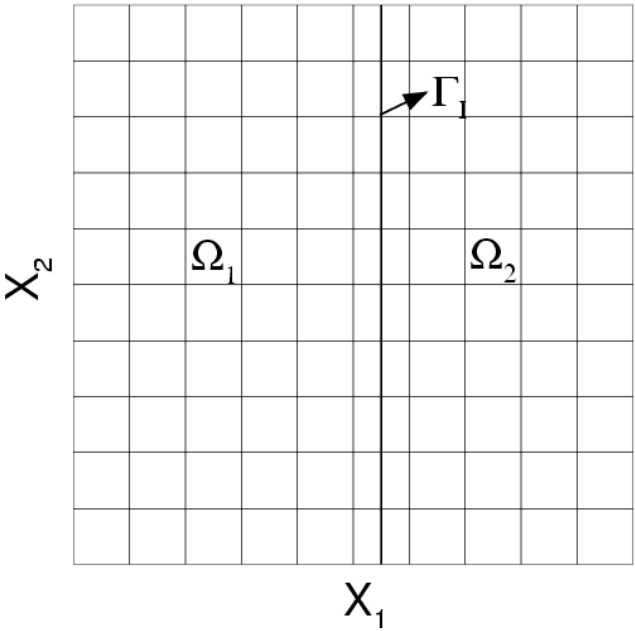
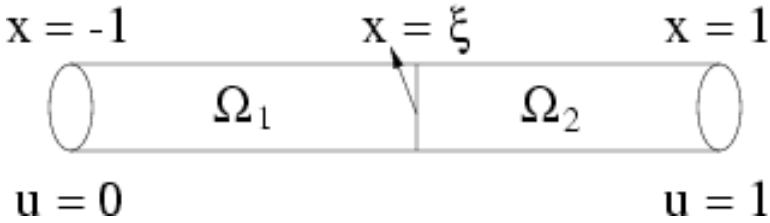
Modeling Holes



Level set function for holes



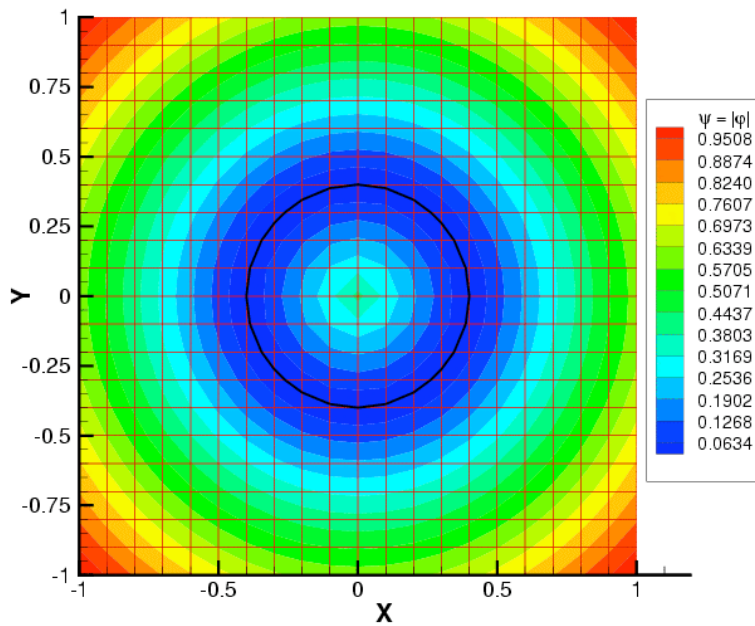
Modeling Weak Discontinuities (1D Bimaterial Bar)



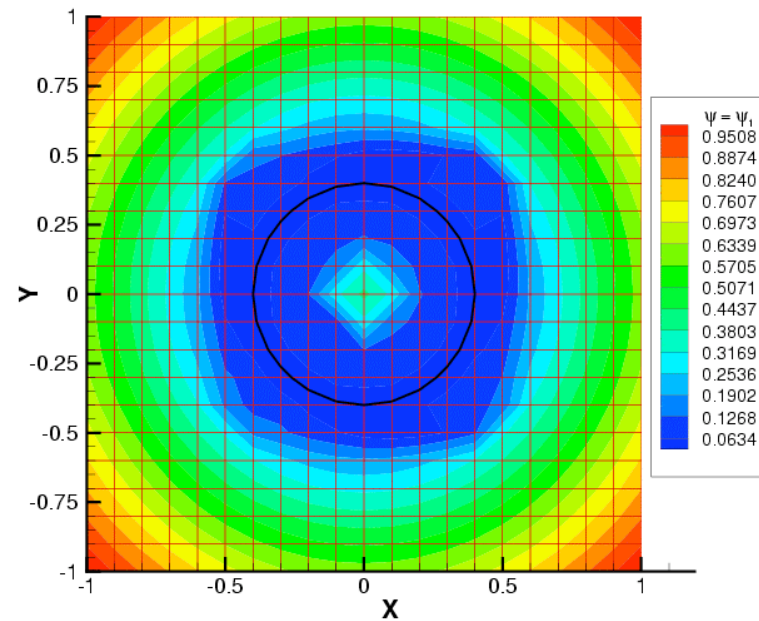
Enrichment Function



Enrichment Functions (2D BVP)



$|\varphi|$

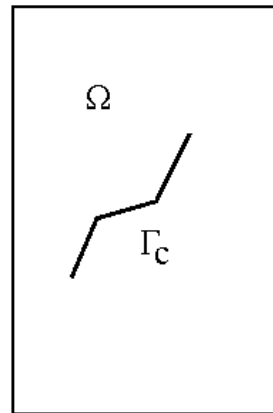


Laplacian smoothing
of φ

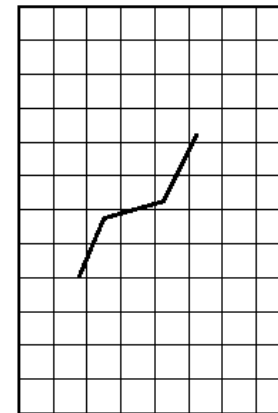


Extended Finite Element Method (X-FEM)

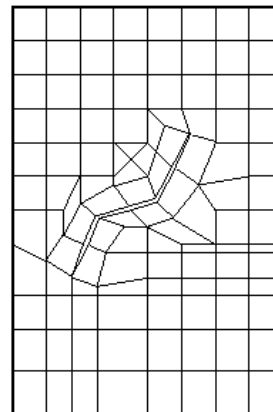
Crack Modeling in 2D (Dolbow, 1999)



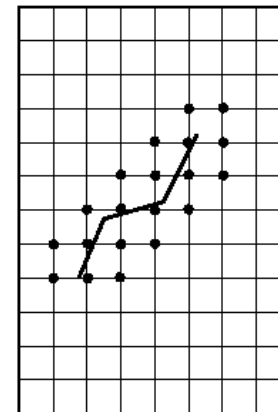
a)



b)



c)



d)



Enriched Displacement Approximation (3D Cracks)

$$u_i^h(\mathbf{x}) = \sum_{n_I \in \mathbf{N}} \phi_I(\mathbf{x}) u_{iI} + \sum_{n_J \in \mathbf{N}^c} \phi_J(\mathbf{x}) a_{iJ} \Psi(\mathbf{x})$$

- **Crack Interior Enrichment:** $\Psi(\mathbf{x})$ is the Heaviside function and \mathbf{N}^c is the set of nodes whose support intersects the crack interior
- **Crack Front Enrichment:** $\Psi(\mathbf{x})$ are the asymptotic crack functions and \mathbf{N}^c is the set of nodes whose support (closure) intersects the crack front



Representation of a Planar Crack

Crack Front

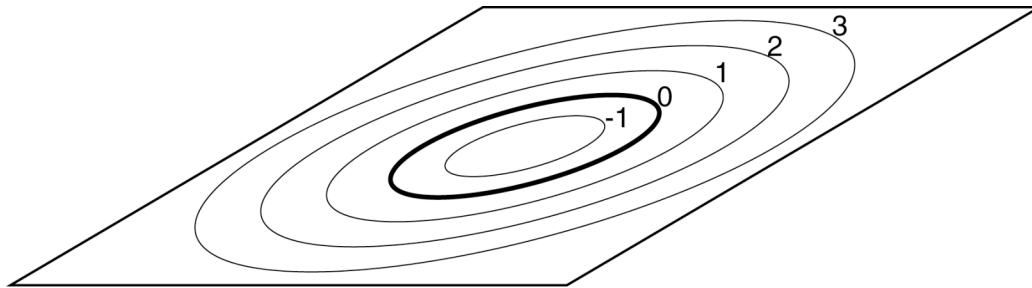
Signed distance function $\varphi_1(\mathbf{x})$ is the distance of \mathbf{x}_p , the orthogonal projection of \mathbf{x} on the crack plane, to the crack front

Crack Plane

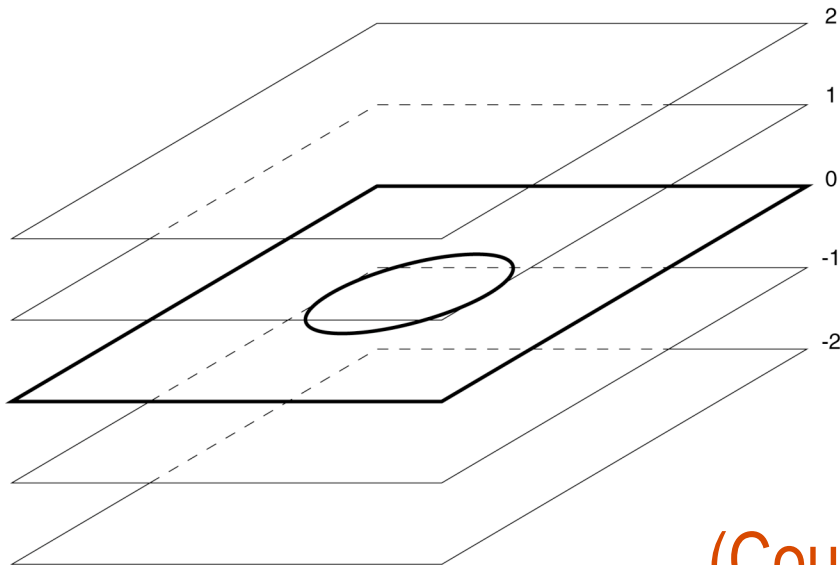
Signed distance function $\varphi_2(\mathbf{x})$ is the signed distance (+ above and - below) to the crack plane



Signed Distance Functions



φ_1

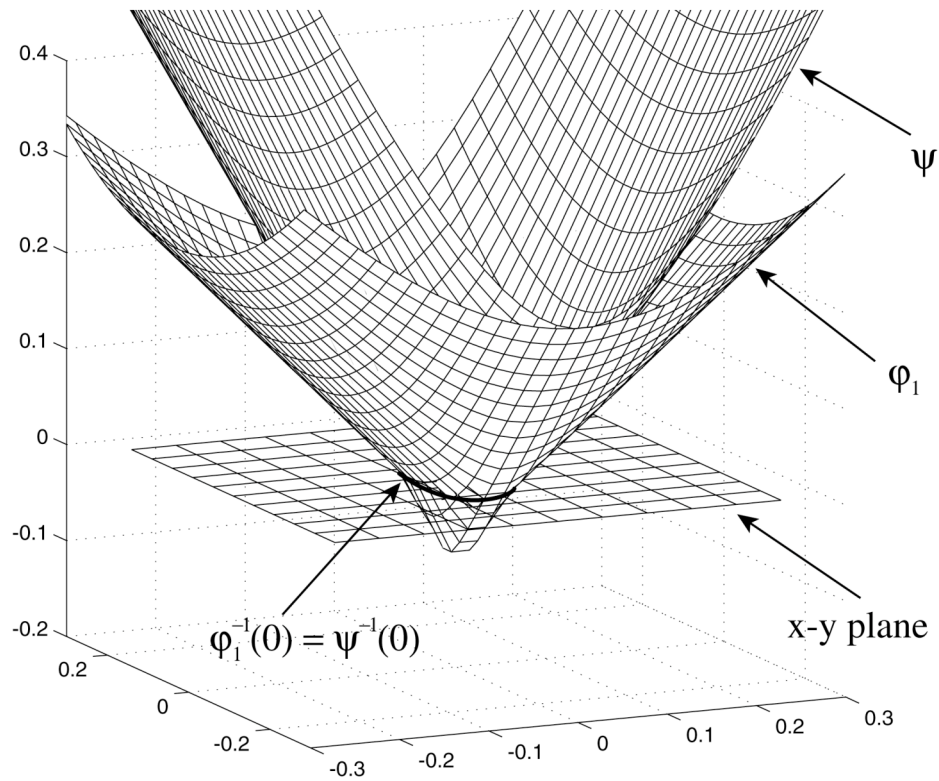


φ_2

(Courtesy of Chopp)



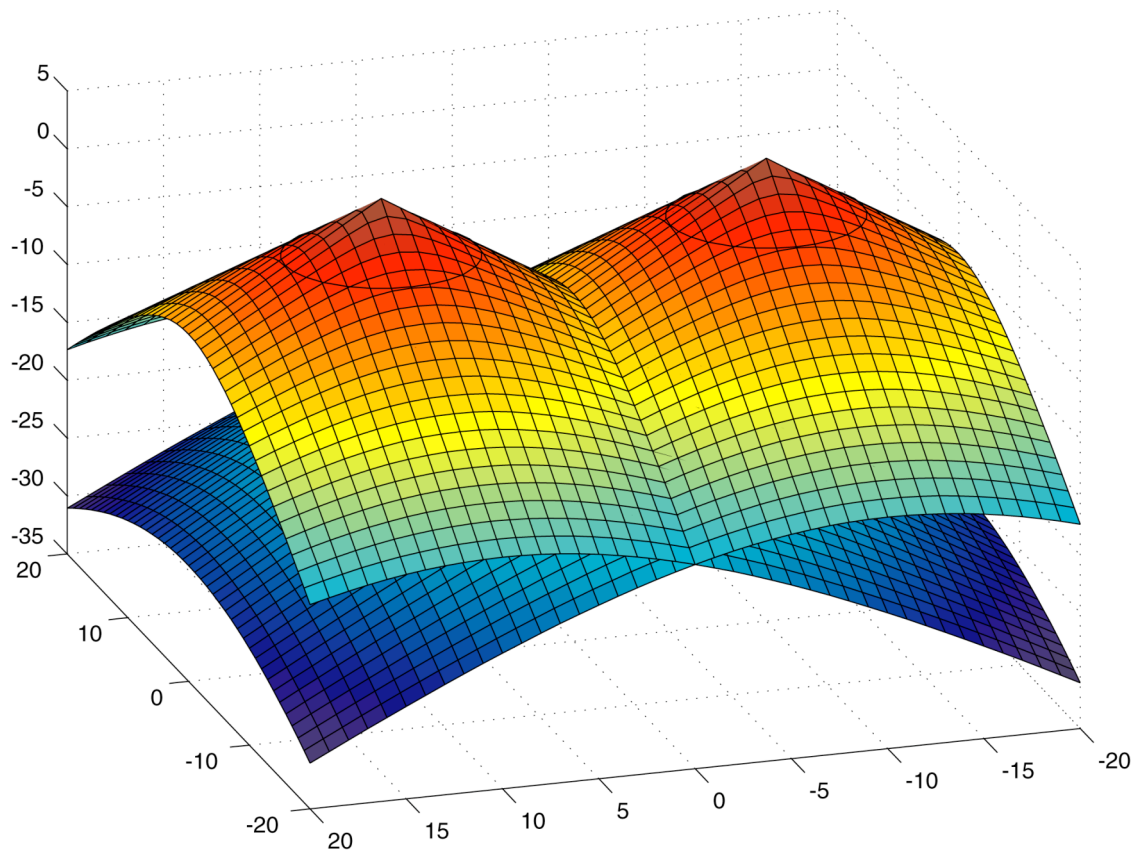
Level Set (ψ) and Signed Distance Function (ϕ_1)



(Courtesy of Chopp)



φ_1 Signed Distance Function (Two Cracks)



(Courtesy of Chopp)



Nodal Enrichment

Selection of Nodes

Nodes are selected for enrichment on the basis of the values of the signed distance functions φ_1 and φ_2

Crack Interior Enrichment

$$H(\mathbf{x}) = \text{sign}(\varphi_2(\mathbf{x}))$$
$$\text{sign}(\xi) = \begin{cases} 1, & \text{if } \xi \geq 0 \\ -1, & \text{otherwise} \end{cases}$$



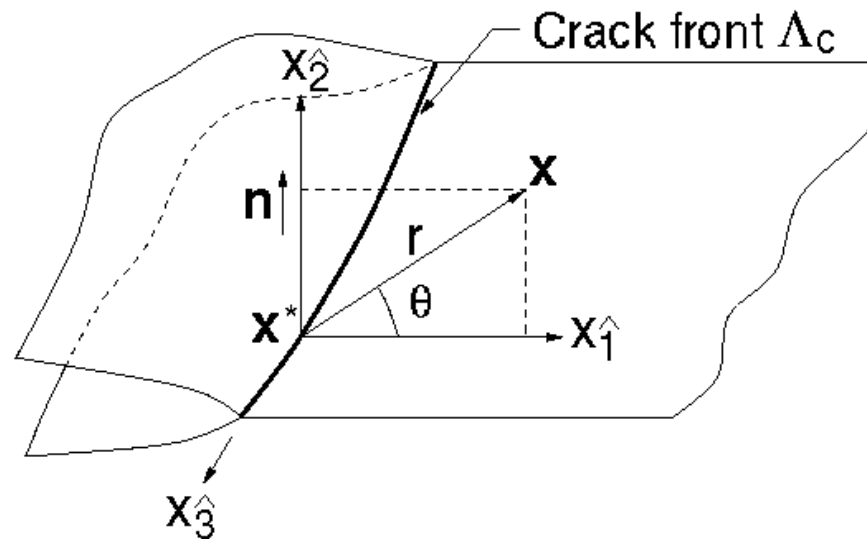
Nodal Enrichment (Cont'd)

Crack Front Enrichment

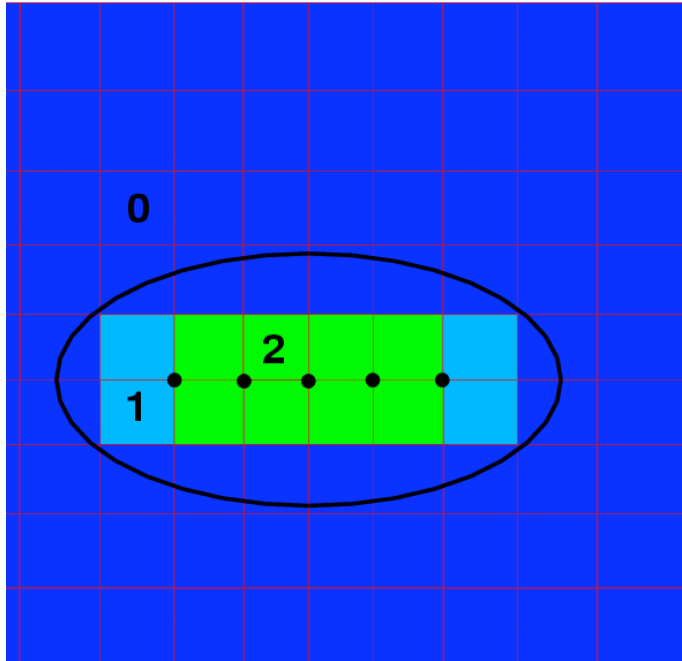
$$\psi = \left\{ \sqrt{r} \cos \frac{\theta}{2}, \sqrt{r} \sin \frac{\theta}{2}, \sqrt{r} \sin \theta \sin \frac{\theta}{2}, \sqrt{r} \sin \theta \cos \frac{\theta}{2} \right\}$$

$$r = \sqrt{\varphi_1^2 + \varphi_2^2}$$

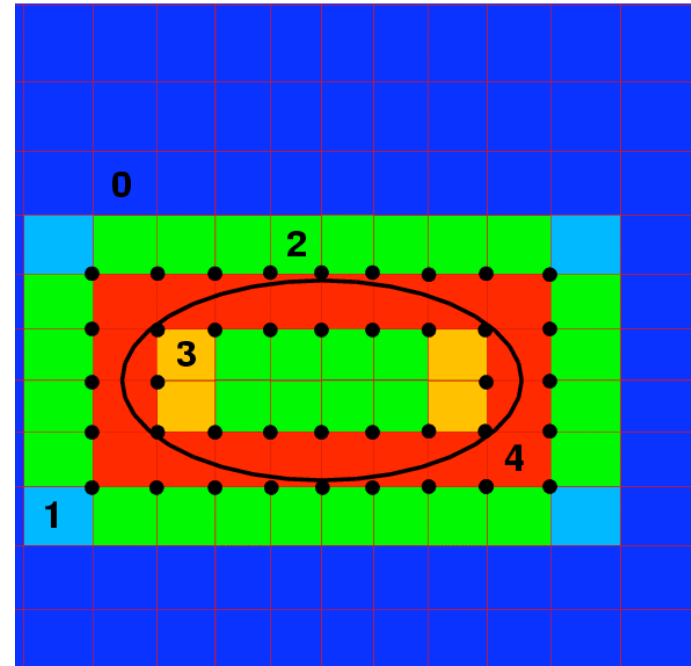
$$\tan \theta = \frac{\varphi_2}{\varphi_1}$$



Nodal Enrichments for Elliptical Crack



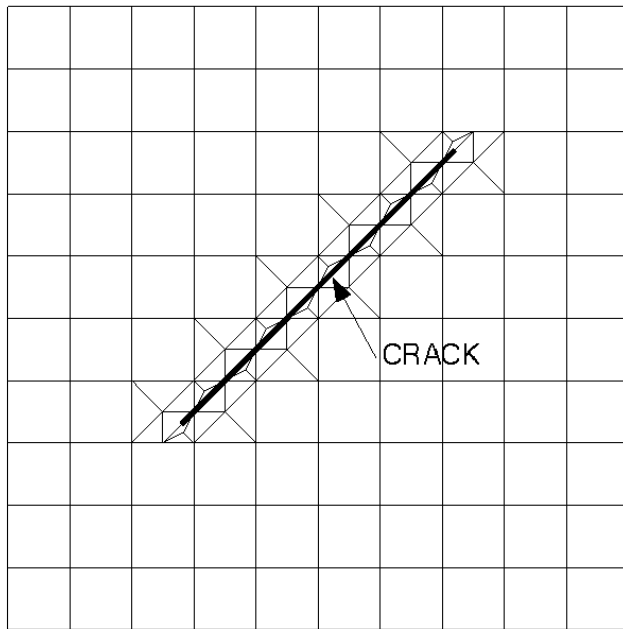
Heaviside Enrichment



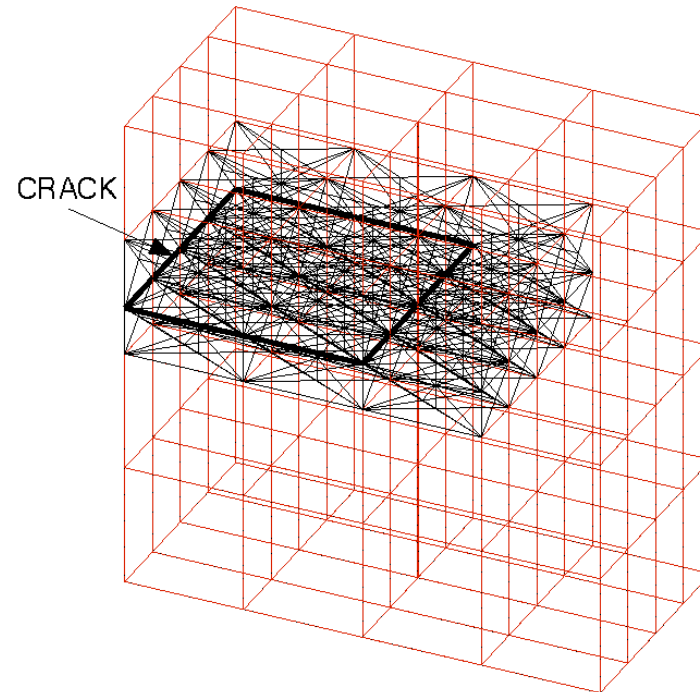
Crack-Front
Enrichment



Partitioning Finite Elements



2D

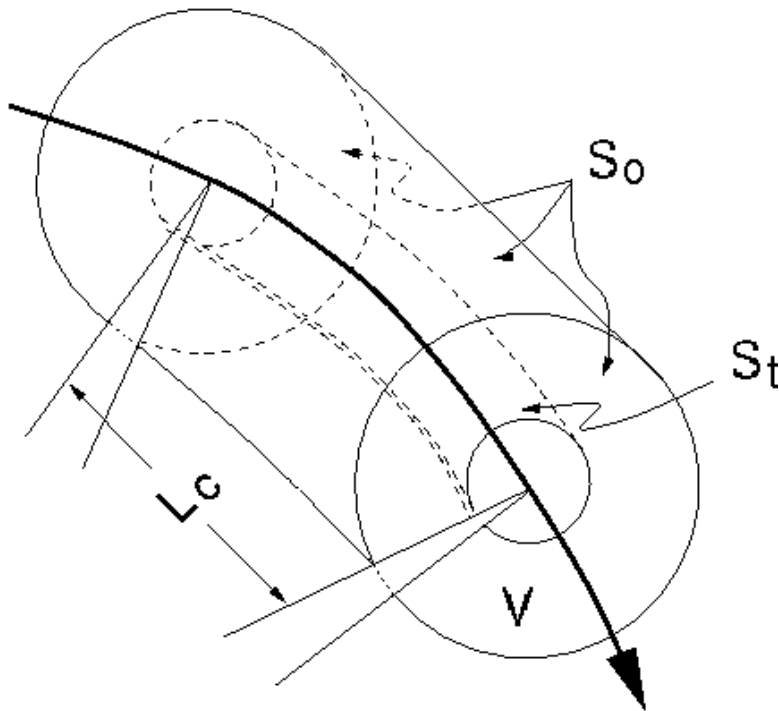


3D



Computation of Stress Intensity Factors

Domain Integrals (Moran and Shih, 1987)

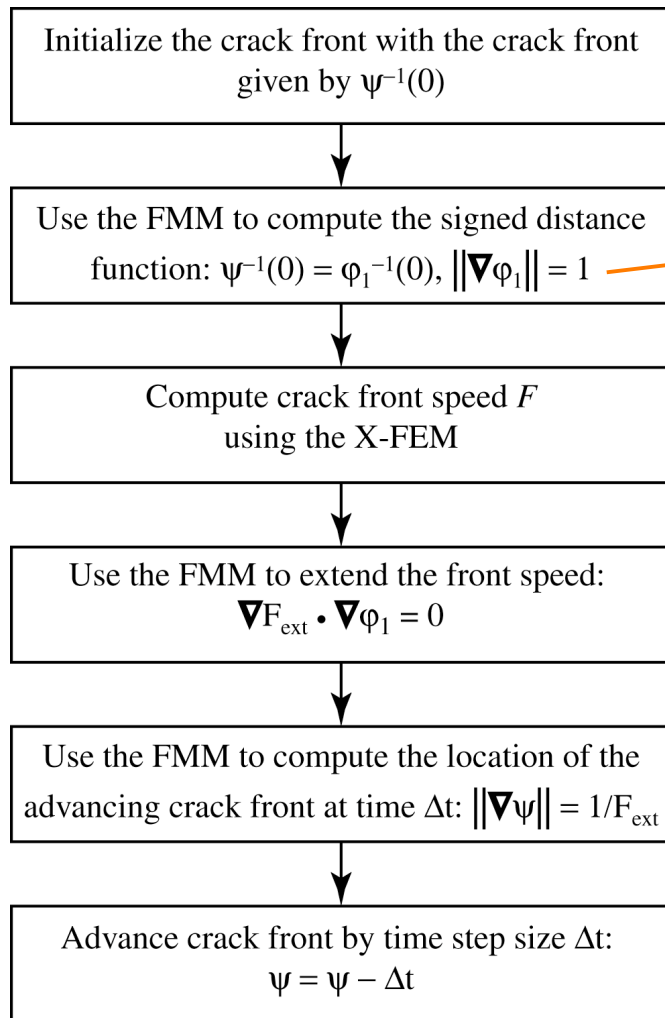


$$K_I(s) = \sqrt{\frac{J(s)E}{1-\nu^2}}$$

$$J(s) = -\frac{\int_V H_{kj} q_{k,j} dV}{\int_{L_c} l_k n_k ds}$$



X-FEM/FMM Crack Growth Algorithm

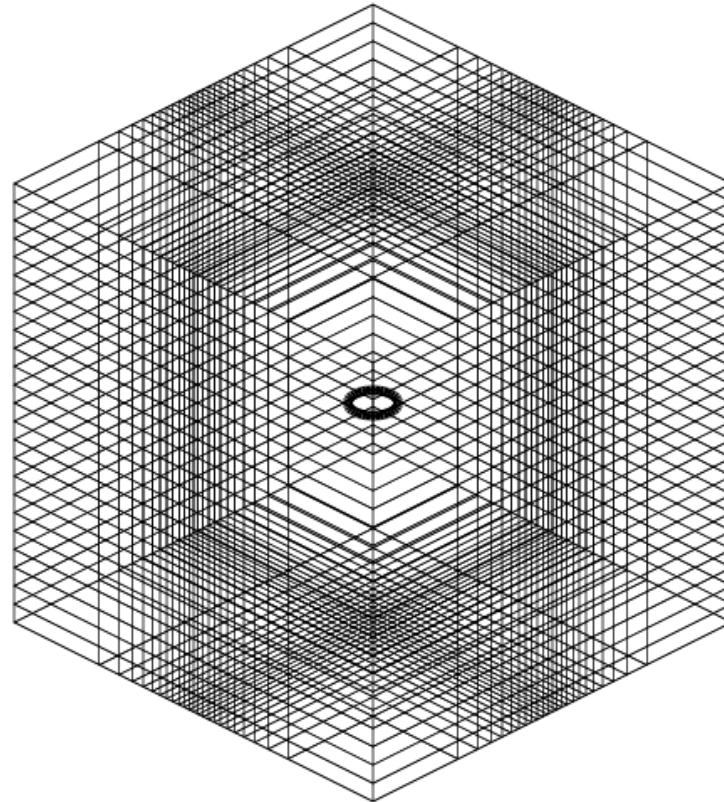


$$\frac{\partial \phi_1}{\partial n} = 1 \Rightarrow \nabla \phi_1 \cdot \mathbf{n} = 1$$
$$\Rightarrow \|\nabla \phi_1\| = 1$$

(Courtesy of Chopp)



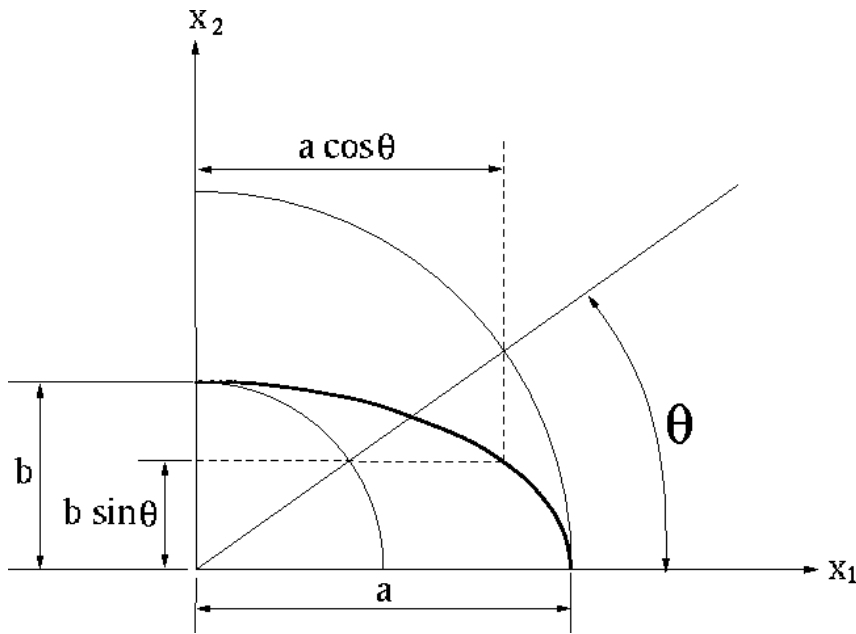
Hexahedral Mesh



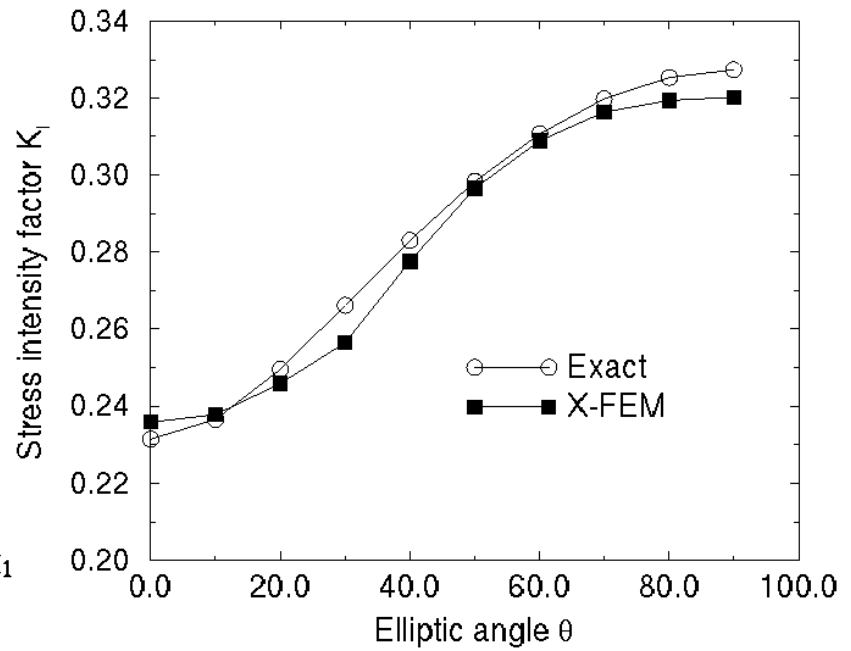
Penny crack (24^3 mesh)



Planar Elliptical Crack



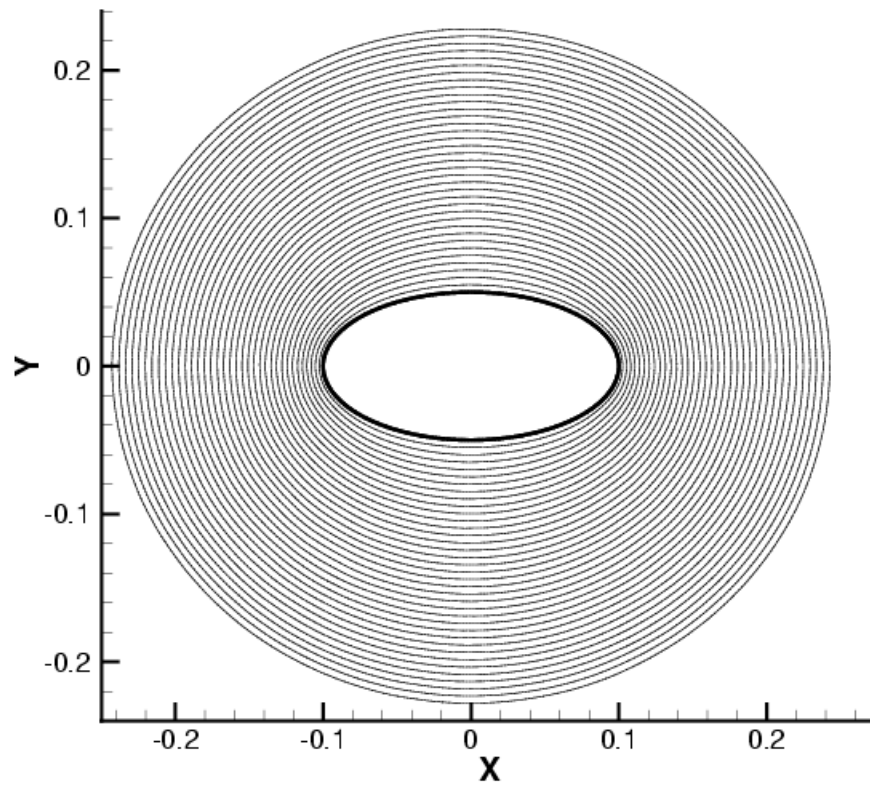
Elliptic angle



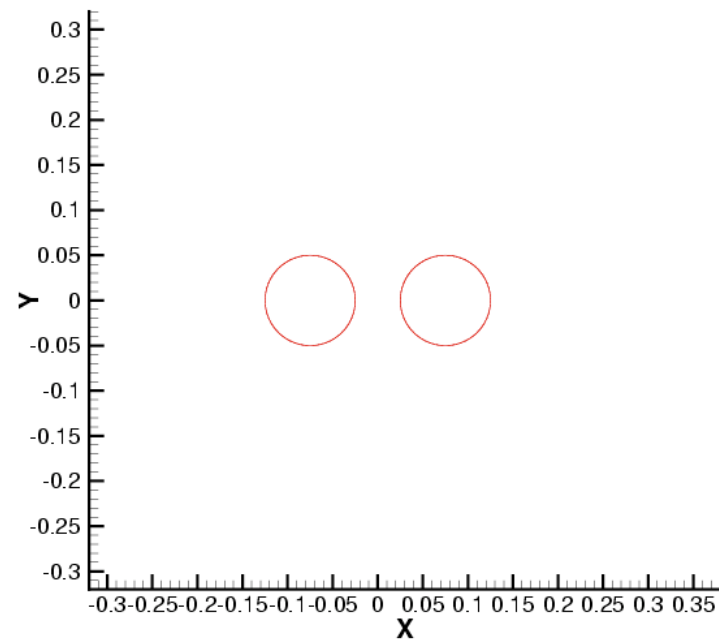
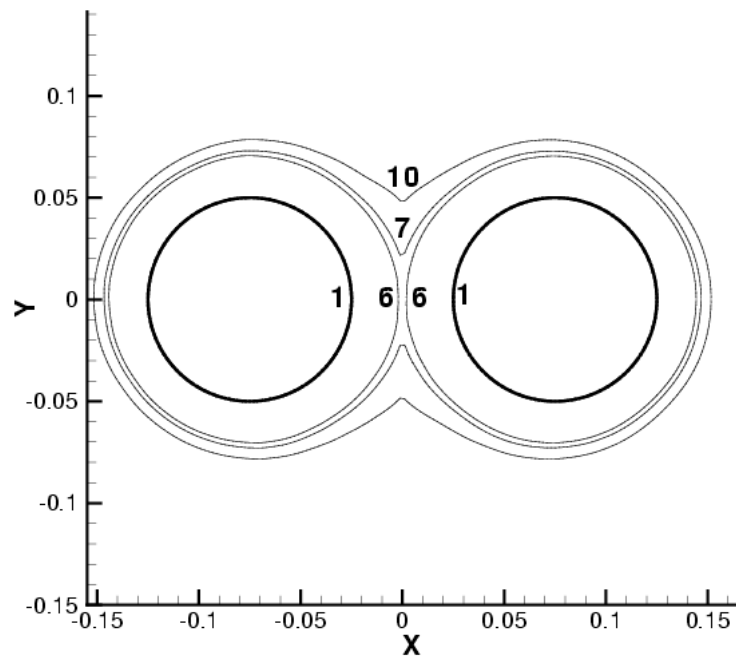
SIFs



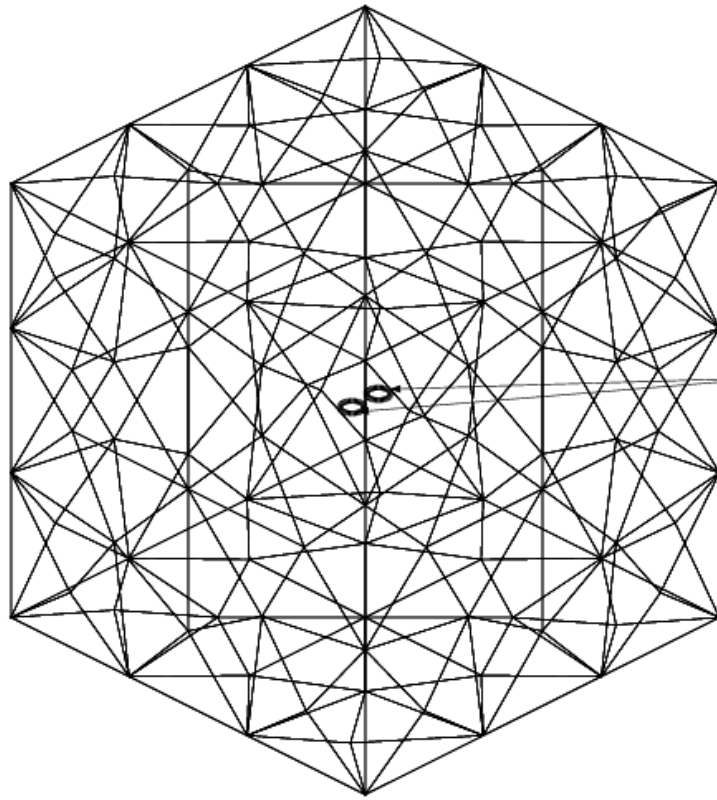
Fatigue Growth of One Elliptical Crack



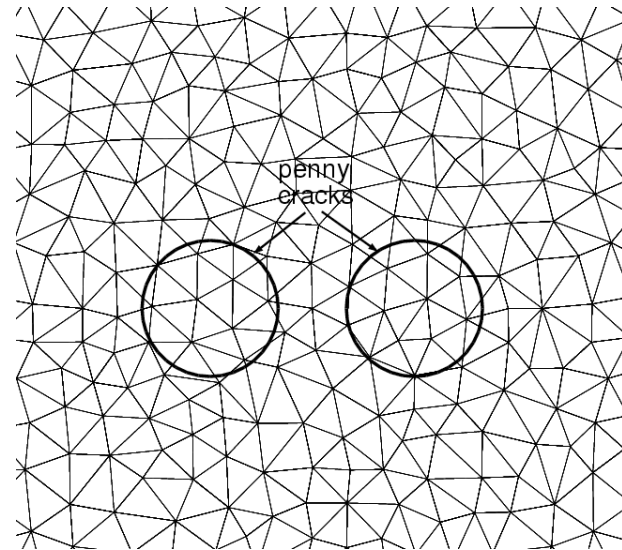
Fatigue Growth of Two Penny Cracks



Tetrahedral Mesh



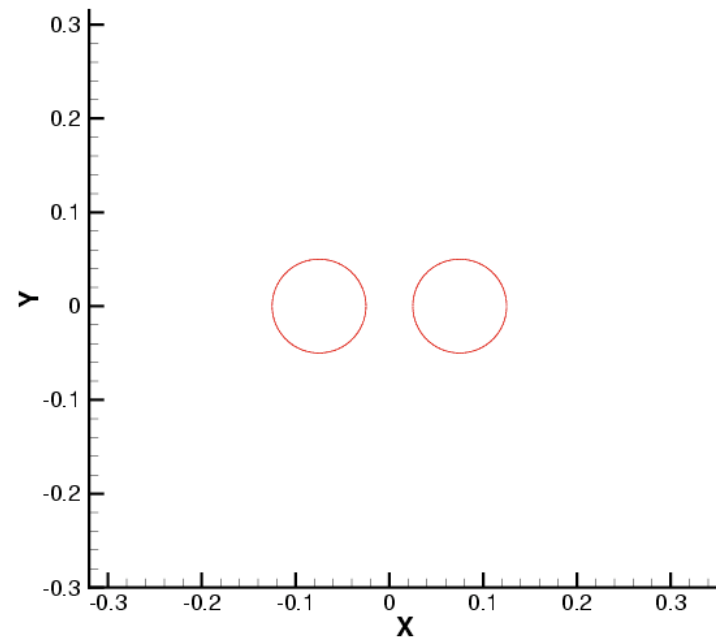
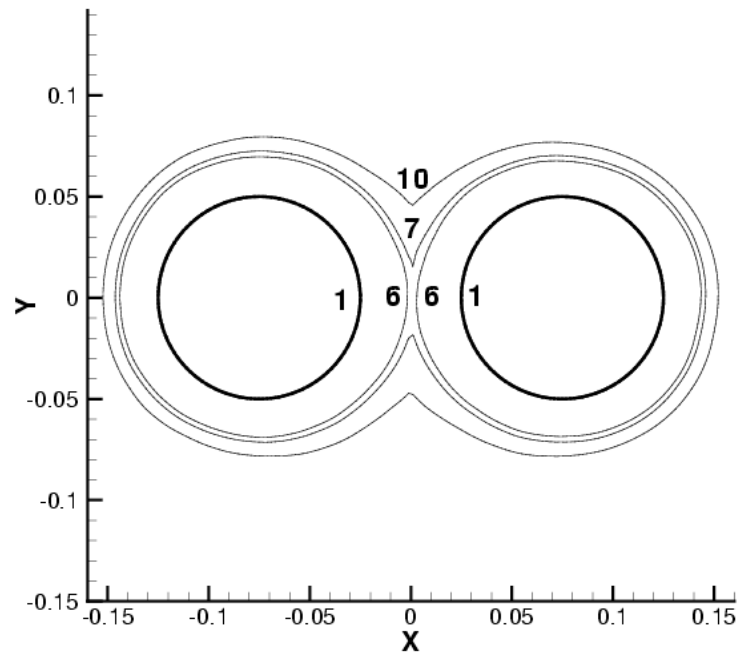
Surface mesh



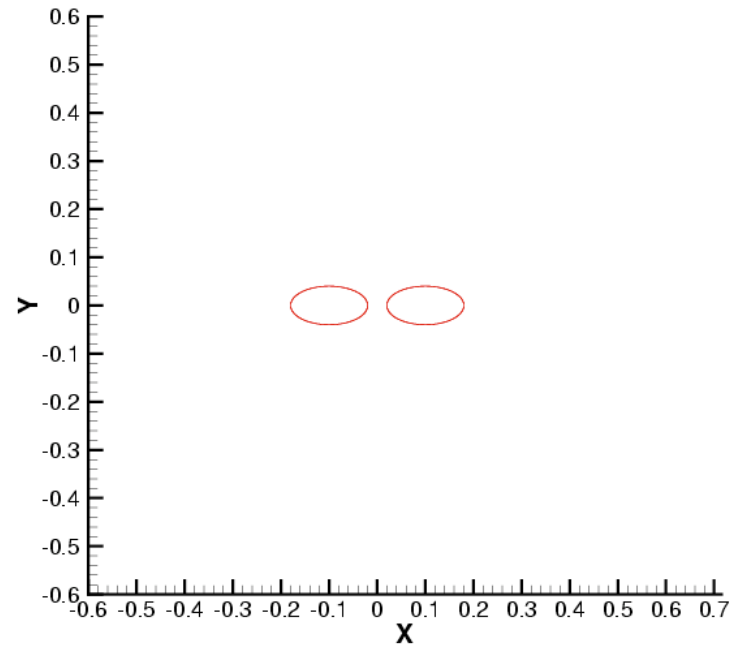
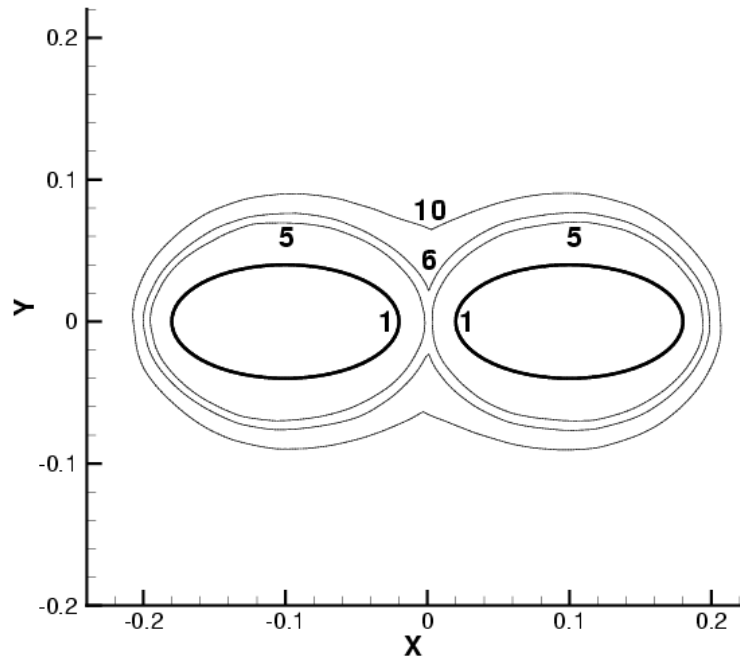
Vicinity of the crack



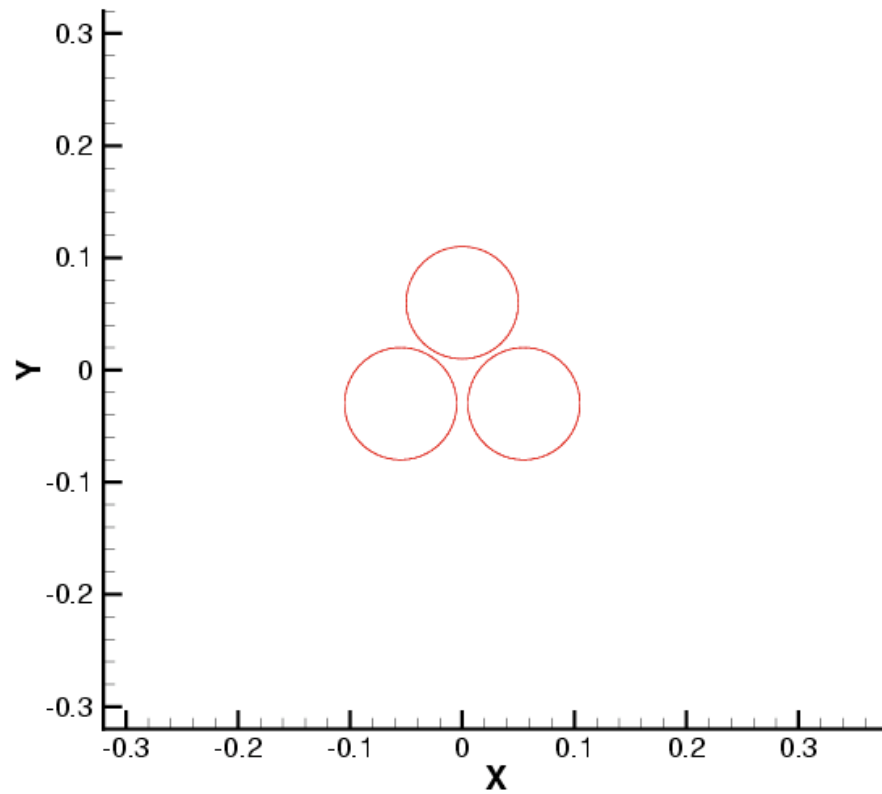
Fatigue Crack Growth (Tetrahedral Mesh)



Fatigue Growth of Two Elliptical Cracks



Fatigue Growth of Three Penny Cracks



Modeling Brittle Fracture in Polycrystals

Lattice Spring Network Models

- **Beale & Srolovitz (1988); Curtin & Scher (1990)**
 - **Yang et al. (1990); Holm (1998)**
 - **Zimmermann et al. (2001)**
- } Potts grain growth model

Cohesive Surface Formulation

- **Zhai and Zhou (2000)**
 - **Zavattieri et al. (2001)**
- } dynamic fracture



Grain Growth Model

Ising Model (Ising, 1925)

- Phase transitions (anti-ferromagnetic \leftrightarrow ferromagnetic)
- A two-spin (parallel and anti-parallel) model

Potts Model (Potts, 1952)

- Phase transitions using Q -degenerate states; identical to the Ising model for $Q = 2$
- Introduced for grain growth evolution and microstructural processes by Srolovitz et al., 1984, 1985

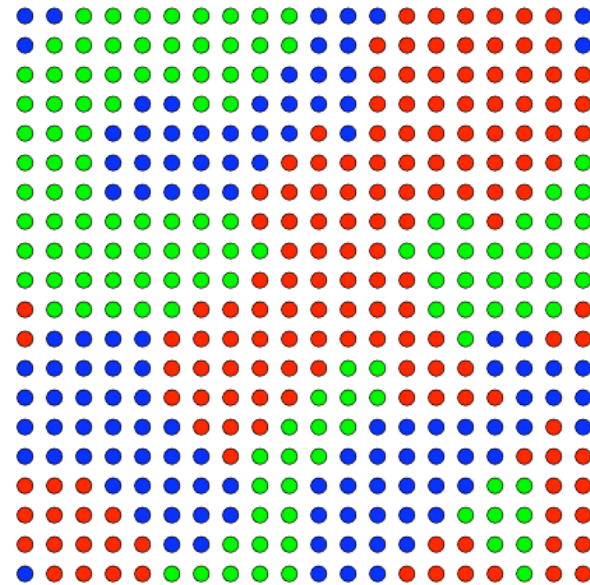


Potts Model

Kinetic Monte Carlo

- Square lattice with N sites
- Q possible spins at each site
- Spin s_i at site i
- Periodic boundary conditions

$$N = 400, Q = 3$$



Potts Hamiltonian

$$H = J \sum_{i=1}^N \sum_{j=1}^{nn(i)} (1 - \delta_{s_i s_j})$$



Microstructure-Meshing

OOF (Carter et al., 1998)

- Microstructure from micrograph or Potts model
- Construction of the FE mesh is directly based on the bonds between adjacent sites in the Potts model

VCFEM (Ghosh et al., 1997)

- Voronoi polygons are used to construct the microstructure as well as to perform the FE analysis

Present Work

- A constrained Delaunay algorithm with smoothing is developed to mesh the microstructure



Constrained Delaunay Triangulation

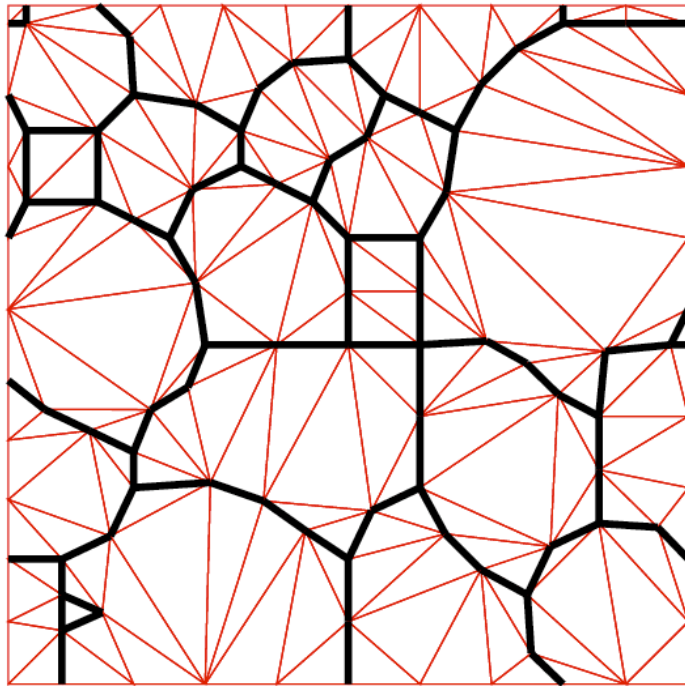
Procedure

- Construct initial boundary conforming triangulation using a cubic least squares polynomial fit to represent the grain boundary edges
- Delaunay refinement using the point insertion algorithm of Rebay (**Rebay, 1993**) is implemented
- Mesh constructed for user-specified spacing ρ

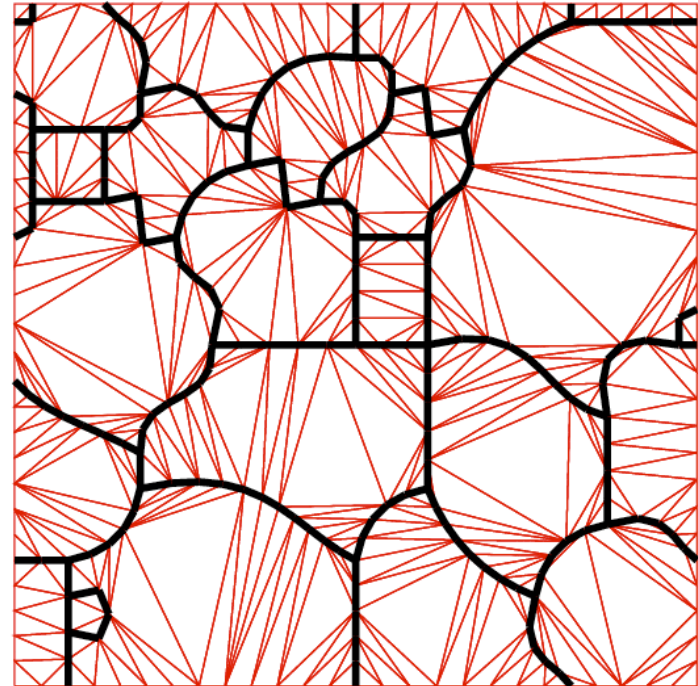


Boundary Conforming Triangulation

N = 400



$\rho = 0.1$

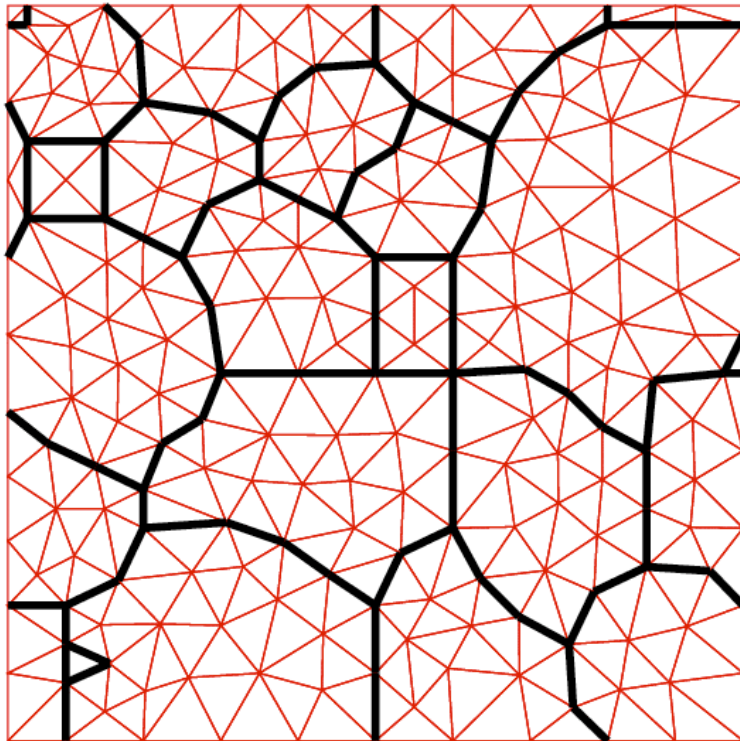


$\rho = 0.04$

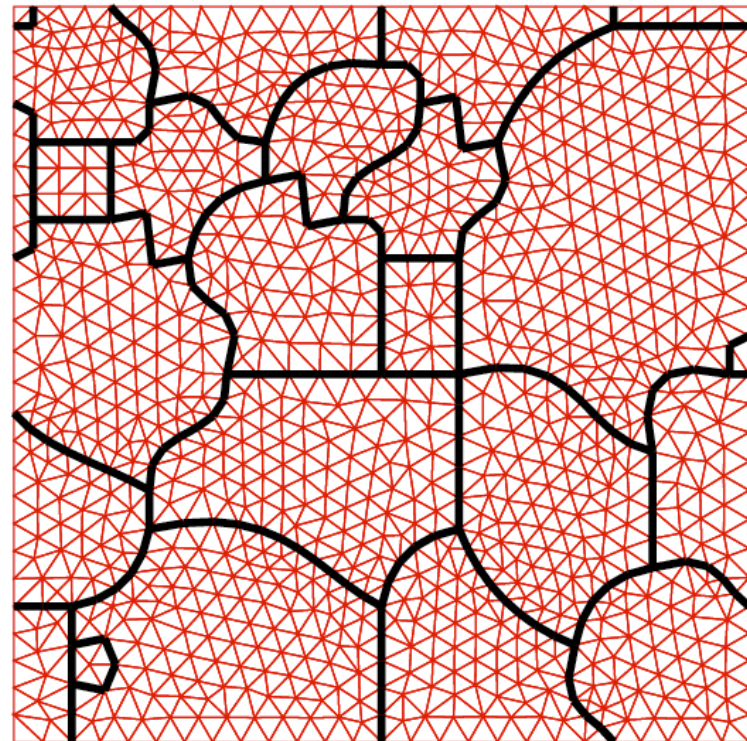
STEP 1



Final Triangulation



$\rho = 0.1$

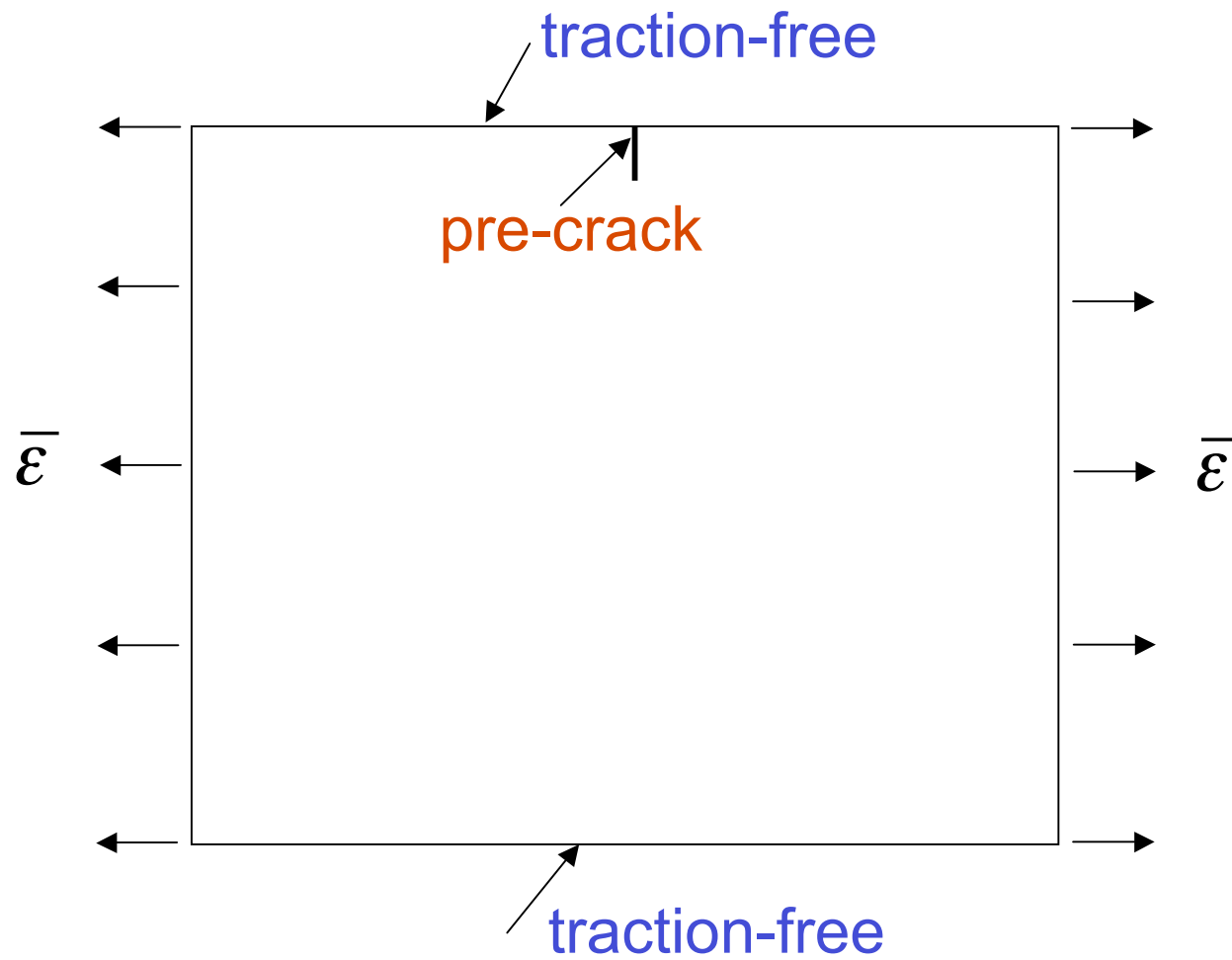


$\rho = 0.04$

STEP 2



Model Geometry and BCs



Simulation Procedure

1. Read parameters: n_{\max} , G_c^i , G_c^{gb} , Δa_{\max}
 $n = 0$; $\bar{\varepsilon}_0 = 1$
2. X-FEM analysis for initial crack-tip location
 $failure = 0$
3. **while** ($n < n_{\max}$ and $!failure$) {
4. $n = n + 1$
 if ($\mathbf{x}_{\text{tip}} \in \Omega_i$)
 $\theta_g = \theta_{\text{hoop}}$; $\Delta a = \min(\Delta a_{\max}, \Delta a_{gb}, \Delta a_{\text{hull}})$

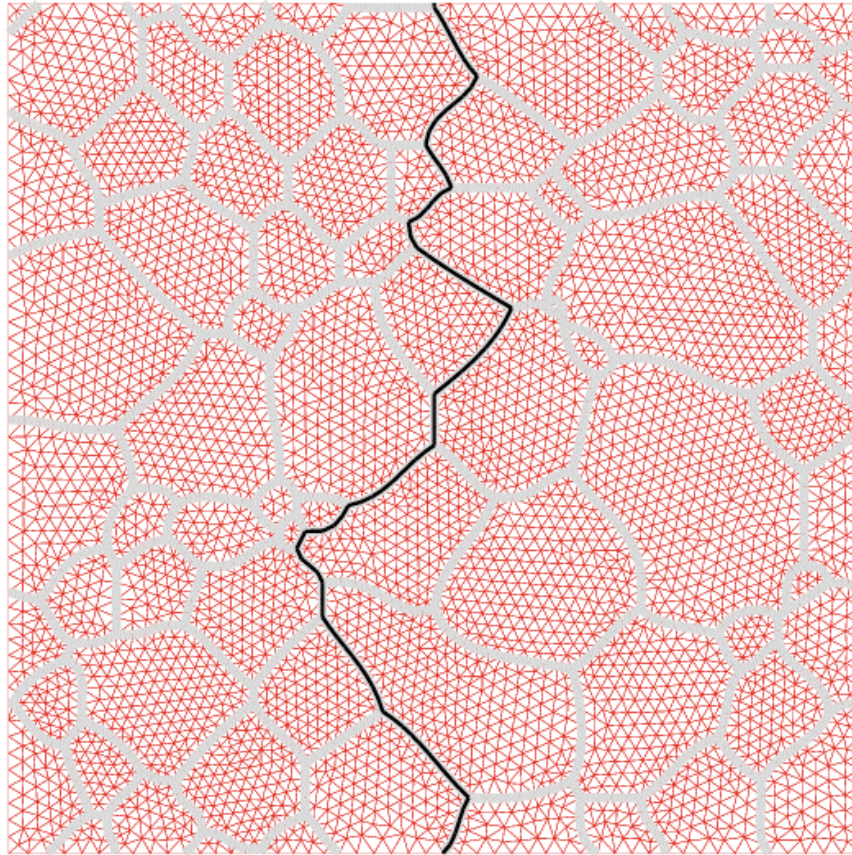


Simulation Procedure (Cont'd)

5. if ($\mathbf{x}_{\text{tip}} \in \Gamma_{gb}$)
 - find grain boundary directions θ_{gb}
 - perturb crack along θ_{gb} and θ_{hoop} and find θ_g based on $\max(G^{gb} / G_c^{gb}, G^i / G_c^i)$
 - $\Delta a = \min(\Delta a_{\text{max}}, \Delta a_{gbv})$
6. critical strain ($G = G_c$): $\bar{\varepsilon}_n = \sqrt{G_c^k / G} \bar{\varepsilon}_{n-1}$
7. determine *failure* status
8. X-FEM analysis with $\bar{\varepsilon}_n$ before and after crack growth
- }
9. end



Crack Propagation Simulations ($Q = 100$)

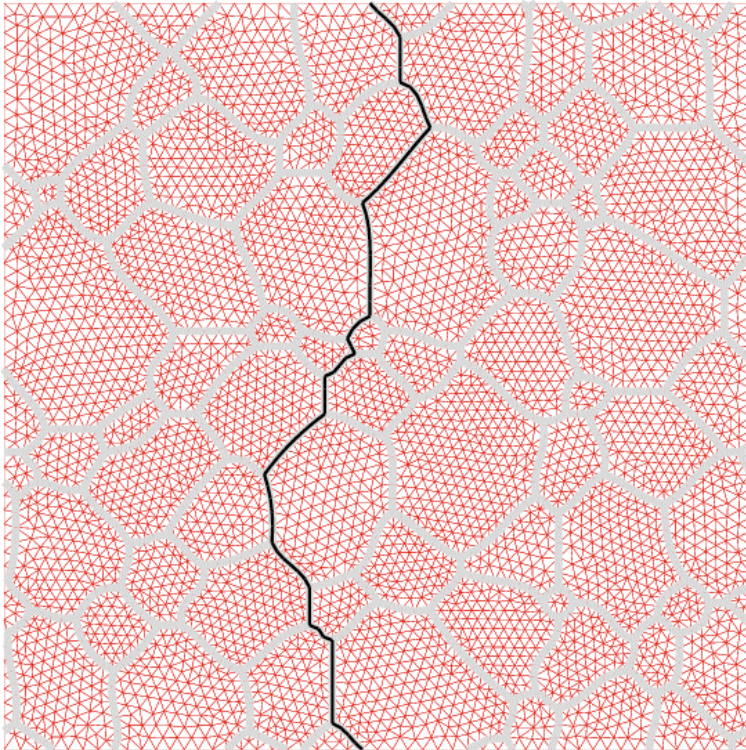


$$G_c^{gb} / G_c^i = 0.1$$
$$t = 10^4 \text{ MCS}$$

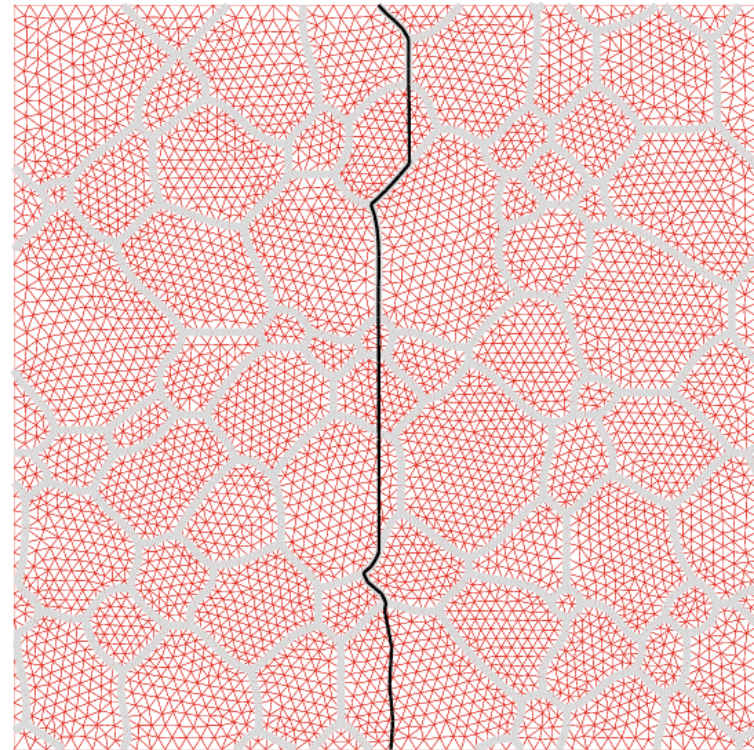
INTERGRANULAR FRACTURE



Simulation 1: $t = 10000$ MCS



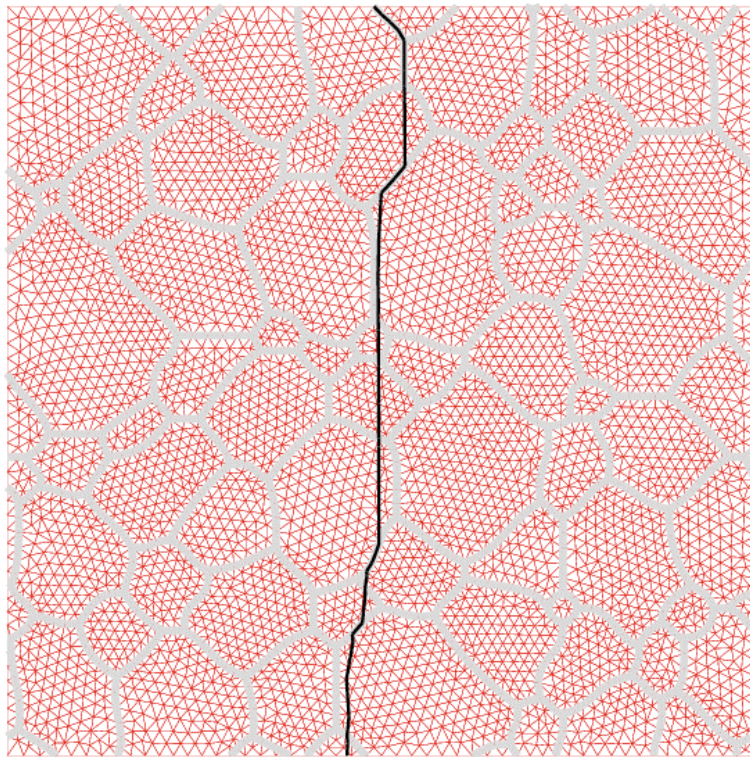
$$G_c^{gb} / G_c^i = 0.3$$
$$IG = 100\%$$



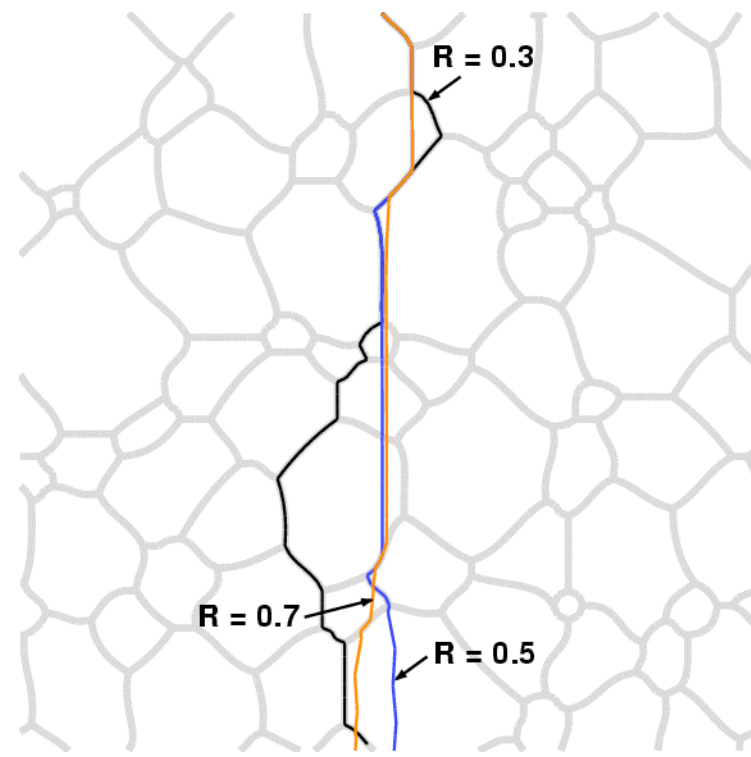
$$G_c^{gb} / G_c^i = 0.5$$
$$IG = 42\%$$



Simulation 1 (Cont'd)



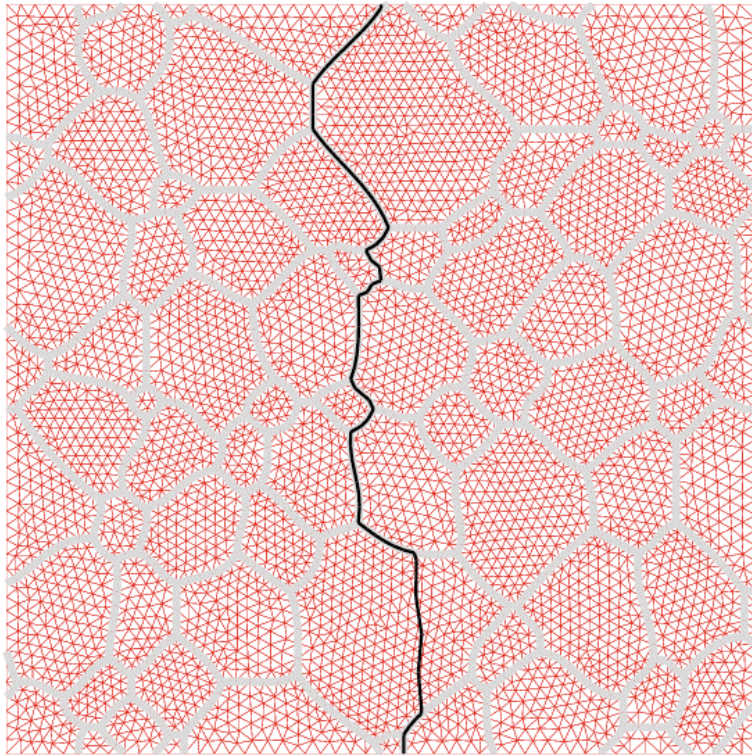
$$G_c^{gb} / G_c^i = 0.7$$
$$IG = 21\%$$



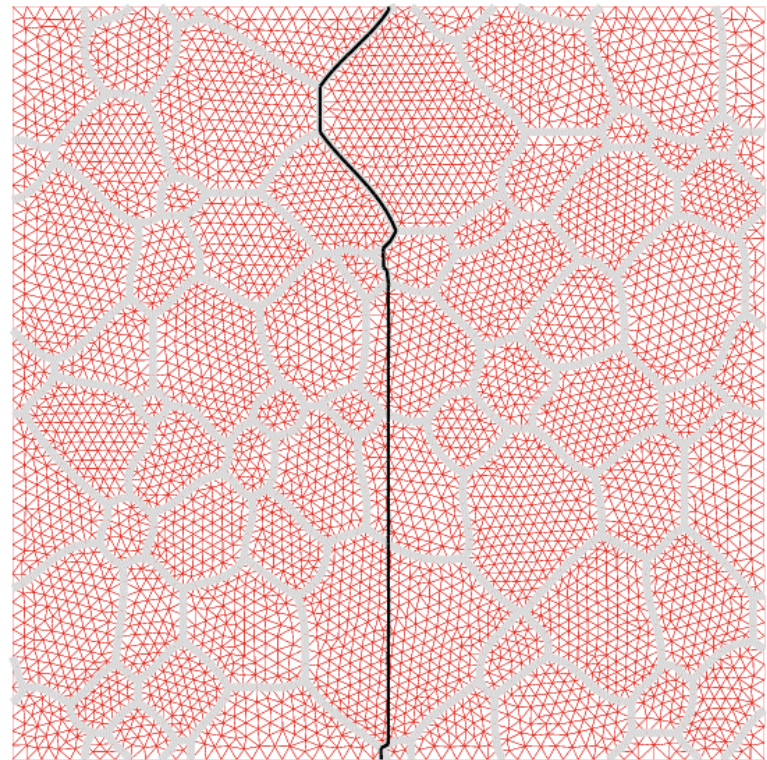
$$R = G_c^{gb} / G_c^i$$



Simulation 2: $t = 10000$ MCS



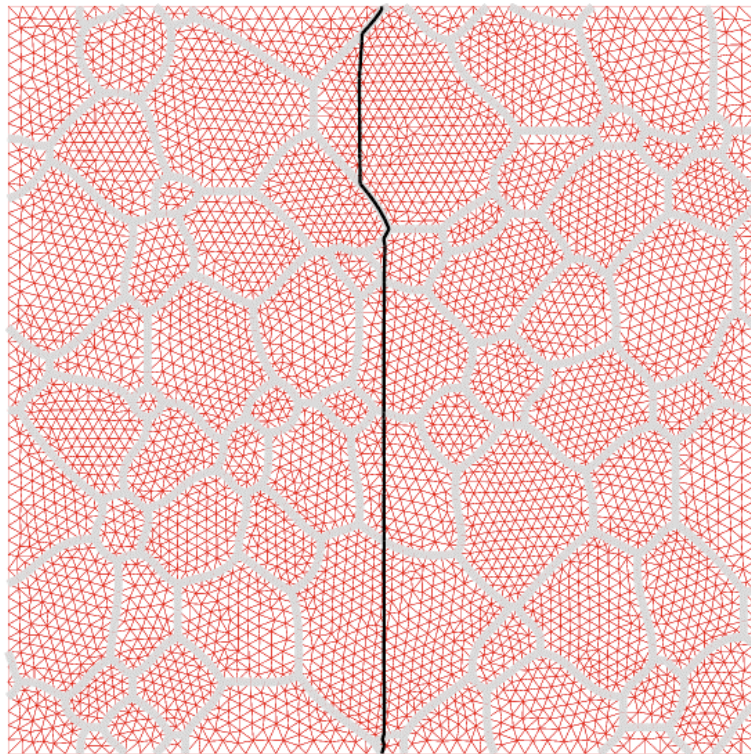
$$G_c^{gb} / G_c^i = 0.3$$
$$IG = 81\%$$



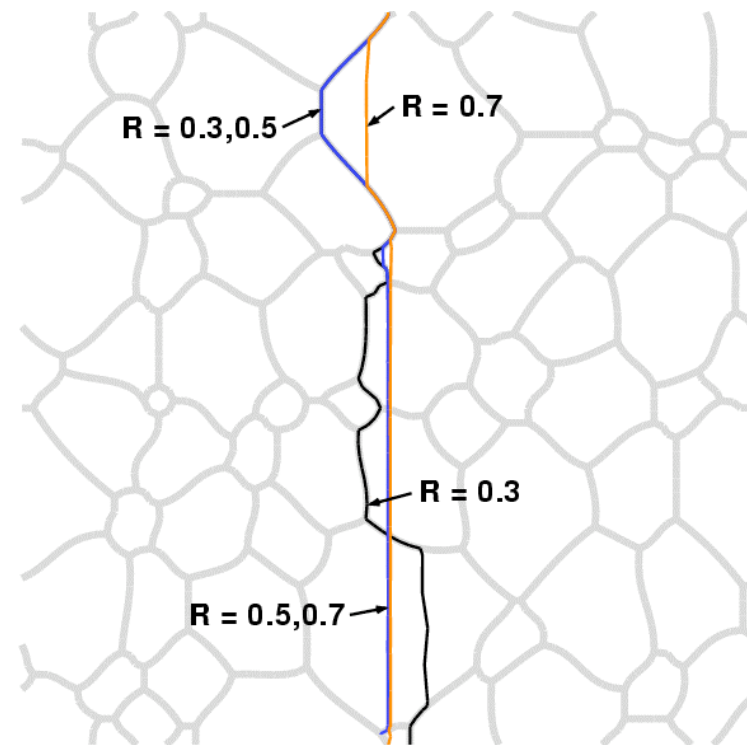
$$G_c^{gb} / G_c^i = 0.5$$
$$IG = 40\%$$



Simulation 2 (Cont'd)



$$G_c^{gb} / G_c^i = 0.7$$
$$IG = 13\%$$



$$R = G_c^{gb} / G_c^i$$



Conclusions

- A numerical technique (**X-FEM**) that can model strong as well as weak (strain) discontinuities within finite elements was introduced
- Level sets and fast marching methods were shown to provide a powerful complement to the X-FEM in tracking the evolution of discontinuities
- Versatility of the X-FEM was demonstrated via various applications: material interfaces, 3-D crack growth, and brittle fracture in polycrystalline materials

